

RESEARCH ARTICLE

Biosynthesis of Silver Nanoparticles using *Rhizophora mucronata* and *Ceriops decandra* and their Antagonistic Activity on Gut Cellulolytic Bacteria

M. Vijaya Sankar*, S. Abideen

Department of Zoology, Dr. Zakir Husain College, Sivagangai, Tamil Nadu, India

Received: 20 February 2019; Revised: 05 April 2019; Accepted: 26 April 2019

ABSTRACT

To find out the bactericidal properties of biosynthesis silver nanoparticles synthesized with *Ceriops decandra* (*C. decandra*) and *Rhizophora mucronata* (*R. mucronata*), aqueous leaf extract against the cellulolytic bacteria isolated from gut of *Macrotermes convolsonarius* a termite species. Further, characterization such as ultraviolet, X-ray diffraction (XRD), Fourier transform infrared (FT-IR), and scanning electron microscopy was analyzed for biosynthesized silver nanoparticles. A total of 16 isolates were collected from gut of termites. Of these, seven bacterial isolates exhibited positive cellulolytic test. The isolated cellulolytic bacterial colonies were subjected to antibacterial assay with synthesized silver nanoparticles of the selected mangrove plants. *C. decandra* showed highest zone of inhibition (16 mm at the concentration of 150 µg/disc) with TGBS15 and *R. mucronata* showed highest zone of inhibition (18 mm at the concentration of 150 µg/disc) with TGBS09. The synthesized silver nanoparticles of *R. mucronata* and *C. decandra* have maximum absorption at 430 and 400 nm. The XRD data showed 2 θ intense values with various degrees such as 25–30°. The FT-IR results revealed prominent peaks in *R. mucronata* showed absorption bands at 3444, 1622, 1384, 1071, and 471 cm⁻¹ and *C. decandra* showed absorption bands at 3606, 3418, 2923, 1069, 474, and 426 cm⁻¹, respectively. The biosynthesis of silver nanoparticles with aqueous leaf extract of *R. mucronata* provides potential source for cellulolytic bacteria of termites.

Keywords: Biosynthesis, cellulolytic bacteria, mangroves, nanoparticles

INTRODUCTION

Termites are very important ecological components in the circulation of organic matter through decomposition of litter and dead woods.^[9,31] They are also harmful pests causing widespread damage to wooden materials.^[5,30] It consists of >2600 species belonging to 280 genus, presently seven known families and 14 subfamilies. Termites are usually feed on dead wood and they can able to digest cellulose with the help of symbiotic microbes.^[24] Termite guts have numerous cellulolytic bacteria which enable to degrade cellulose. These bacterial populations maintain symbiotic relationships to termites.^[32] Some of the researchers also have pointed out that the termites are most devastating insects, harshly damage agricultural field, and urban infrastructure. In India, termites cause great economic loss in agriculture field.^[11,23,33]

Extensive use of chemical pesticides causes resistance in the termites and toxicity to plants and environment. It risks upon human and animal health resulting into various modern diseases (cancer, Parkinson's, paralysis, abnormal infants and birth rate, increasing pregnancy risks, low weight childbirth, improper memory and mental development, abnormal reflexes, mental and emotional problems, etc.). In the view of toxic effects of chemical pesticides, the plant depend pesticides have emerged as harmless, effectual, and eco-friendly. Plants parts including leaves, stem, bark, seed, and oil contain numerous bioactive compounds such as alkaloids, flavonoids, glycosides, phenols, terpenoids, and tannins. Nanoparticles are considered to be the basic building blocks of nanotechnology.^[18] Nanoparticles taken out from plants source can able to successfully change chemical reduction processes and are considered being eco-friendly; the plants are easily available, harmless to handle and have a wide range of metabolites.^[8,16,17] Several authors have reported anti-termite property

***Corresponding Author:**

M. Vijaya Sankar,

E-mail: vjsankar5@gmail.com

using biosynthesized nanoparticles obtained from terrestrial sources.^[1,3,4,13,26,27,32] However, cellulolytic bacteria which reside inside gut of termites using marine plants synthesized nanoparticle are not studied so far. Hence, the present study was made an attempt to find out the bactericidal properties of biosynthesis nanoparticle using mangrove plants.

MATERIALS AND METHODS

Collection of mangrove plants species

Two mangrove plants species, namely *Ceriops decandra* and *Rhizophora mucronata*, were collected from Karankadu mangrove swamp region (Latitude: 9° 38' N and longitude 78° 57' E) in Ramanathapuram district, Tamil Nadu, South East Coast of India. The taxonomic identification of mangrove plants was authenticated by Prof. Dr. S. Ravikumar, Department of Oceanography and Coastal Area Studies, Alagappa University, Thondi Campus, and the voucher specimen (ZHCCD01 and ZHCCRM02) kept in our research laboratory for further reference.

Biosynthesis of silver nanoparticles

The collected mangrove plant leaves were washed thrice with tap water and twice with distilled water to eliminate adhering soil and salt particles. About 10 g of thinly cut leaves was put in 100 ml of double sterilized distilled water and boiled the mixture for 5 min. The boiled extract was filtered through Whatman no. 1 filter paper and the supernatant was used and stored for further use. A total of 10 ml of collected filtrate were treated with 90 ml of silver nitrate aqueous solution (21.2 g of AgNO₃ powder in 125 mL of Milli Q water) and incubated at room temperature for 10 min, resulting in the formation of brownish-yellow solution, indicating the synthesis of silver nanoparticles.^[20]

Characterization of biosynthesized silver nanoparticles

About 1 ml of solution (diluted with 1:20 v/v Milli Q water) was monitored in ultraviolet-visible (UV-Vis) spectrophotometer (between 300 and 700 nm ranges with 5 nm intervals) with different time intervals (15 min, 30 min, 4 h, 6 h, and 8 h). After 8 h of incubation, the solution

was centrifuged with 12,000 rpm for 20 min and their pellets were redispersed in sterile distilled water. The centrifugation and redispersion were repeated 3 times to ensure the complete separation of nanoparticles. The purified pellet was dried and subjected to the Fourier-transform infrared (FT-IR) spectroscopy measurement in the diffuse reflectance mode at a resolution of 4 cm⁻¹ in KBr pellets. The dried mixture of silver nanoparticles was further analyzed with X-ray diffractometer (X-RD) operated at a voltage of 40 kV and a current of 30 mA with Cu K_α radiation in a 0–20 configuration. In addition, a thin film of sample was also prepared in the coverslip with the 100 μL of the synthesized silver nanoparticles solution and allowed to dry for 5 min and the slides were analyzed with scanning electron microscope (SEM).^[7]

Collection of termite species and isolation of gut bacterial colonies

The termite species *Macrotermes convolsonianus* were taken out from their nest by hand picking method in a sterilized Petri plate at Dr. Zakir Husain College Campus, Ilayangudi, Sivagangai district, Tamil Nadu, India. The species level identification was done as per the identification keys manual of Bose and Premalatha and Rajavel^[6,22] and identified termites were named as TGBS01–TGBS16 (T = Termites, G = Gut, B = bacteria, and S = serial number). The collected species were brought into the laboratory for isolation of gut bacteria. They were then surface sterilized by washing with 70% alcohol. The cellulolytic bacterial serial dilution and isolation were examined by the following standard procedure.^[25]

Test for cellulolytic assay

After isolation, the bacterial strains were allowed to grow in nutrient agar plates where prepared with 1% carboxymethyl cellulose. Strains were streaked onto agar media plates and kept in incubated at 37°C for 48 h. Then, the Petri plates were flooded with 0.1% Congo red reagent and left it for 20 min. Then, the plates were washed with 1 M NaCl. Clearance zones called halo zones were observed against the red color of Congo red for the positive test. The clear zone of inhibition was calculated by the mean zone diameter subtracted into mean

colony diameter. The zone of inhibition ratio of all the cellulolytic bacterial colonies was calculated by mean zone diameter divided into mean colony diameter for both 24 and 48 h.

Antibacterial assay

Filter paper disc method was utilized for testing of biosynthesized silver nanoparticle of mangrove plants *C. decandra* and *R. mucronata* against cellulolytic bacteria collected from the gut of termites *M. convolsionarius*. Whatman No.1 filter paper disc (6 mm diameter) was impregnated with silver nanoparticles at different concentrations of 50 µg, 100 µg, and 150 µg/disc, respectively, and disc was placed onto a nutrient agar plate which was previously wiped down with cellulolytic bacterial strains. All plates were incubated at 37°C under static conditions. After 24 h, the zone of inhibition appearing around the discs was calculated and noted in millimeter diameter. Triplicates were retained for each bacterial strain.

RESULTS

Two mangrove plant species *C. decandra* and *R. mucronata* were used to synthesized

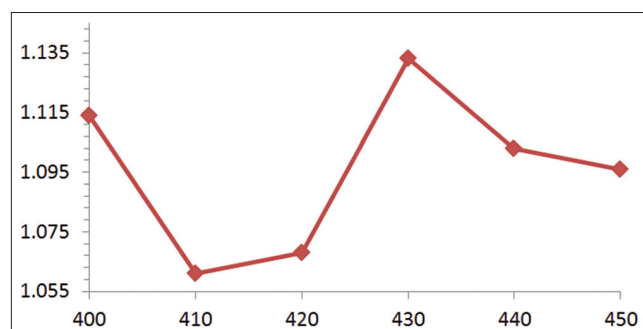


Figure 1: Ultraviolet-visible absorbance peak of *Ceriops decandra* synthesized nanoparticles

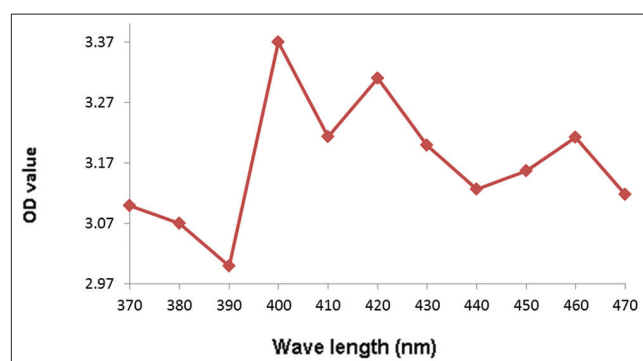


Figure 2: Ultraviolet-visible absorbance peak of *Rhizophora mucronata* synthesized nanoparticles

nanoparticles and used to anti-termite activity. The extracts of mangrove species *C. decandra* and *R. mucronata* color changed to dark brown after the treatment with AgNO_3 . This is due to the property of quantum confinement. The UV-Vis spectrum results showed that the surface plasmon absorption of *C. decandra* band with maximum of 430 nm and *R. mucronata* band with 400 nm. The Figures 1 and 2 showed that the presence of spherical silver nanoparticles *Rhizophora mucronata* and *Ceriops decandra* extracts. This structure was additionally confirmed by SEM images [Figures 3 and 4].

The X-ray diffraction (XRD) curve confirmed that the nanoparticles are nothing but silver. Interpretation of this XRD pattern reveals the existence of diffraction lines at low angles (5° – 75°). The silver nanoparticles biosynthesized from *C. decandra* showed the two peaks of silver at 25 – 35° that can be assigned to the (42) and (100) facets of silver. The silver nanoparticles biosynthesized from *R. mucronata* showed the

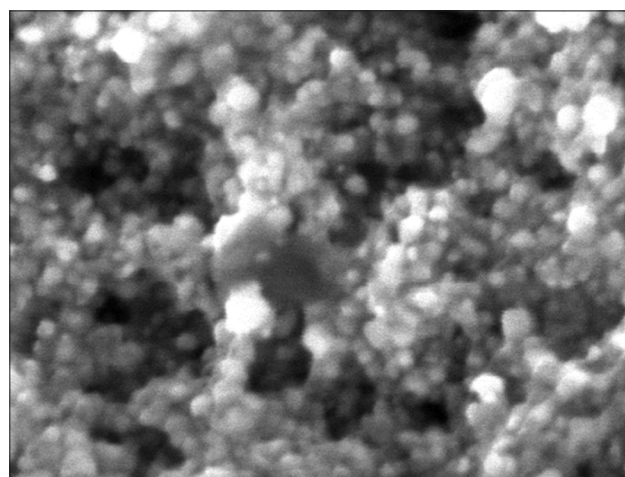


Figure 3: Scanning electron microscope image of *Ceriops decandra*

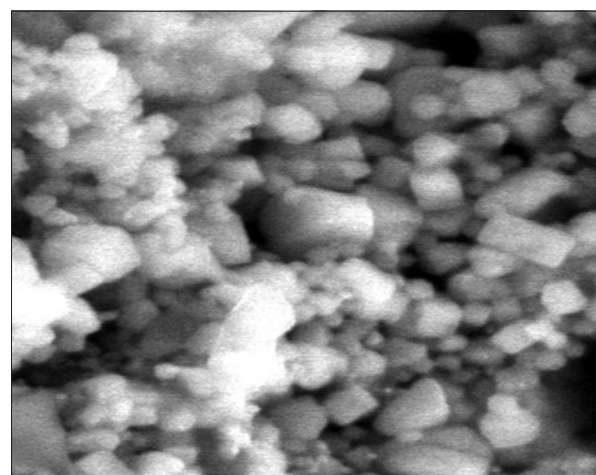


Figure 4: Scanning electron microscope image of *Rhizophora mucronata*

two peaks of silver at 25–35° that can be assigned to the (35) and (100) facets of silver, respectively, which go very well with the many more values

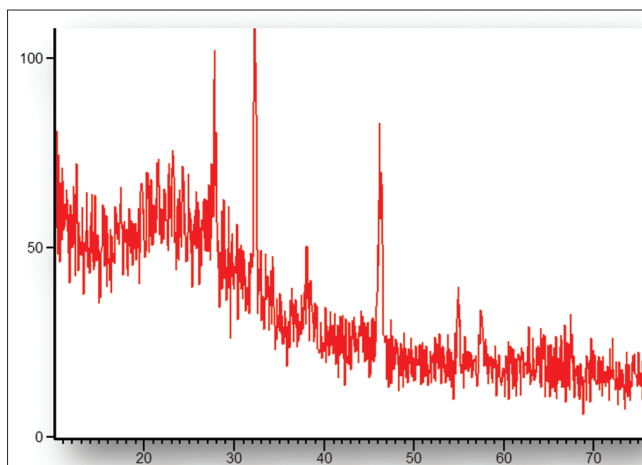


Figure 5: The X-ray diffraction pattern of *Ceriops decandra*

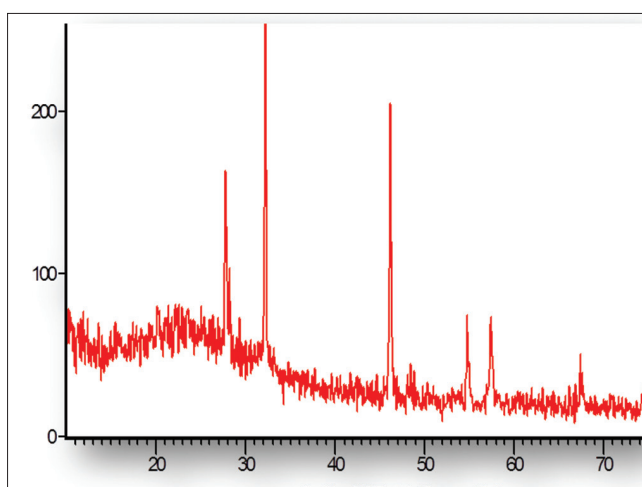


Figure 6: The X-ray diffraction pattern of *Rhizophora mucronata*

manipulated for face-centered cubic structure of silver nanocrystals (according to JCPDS: File No. 4–783) [Figures 5 and 6].

R. mucronata FT-IR spectrum showed absorption bands at 3444, 1622, 1384, 1071, and 471 cm^{-1} , indicating the occurrence of capping agent with the nanoparticles and the image of *C. decandra* FT-IR spectrum showed absorption bands at 3606, 3418, 2923, 1069, 474, and 426 cm^{-1} , respectively [Figures 7 and 8].

In the present study also made an attempt to isolate the gut bacteria from a termite species *M. convolsonianus*. A total of 16 bacterial isolates were collected based on their morphological features and named as TGBS01 to TGBS16, respectively. The maximum colonies count observed in TGBS06 and minimum colonies count noted in TGBS11 and results depicted in Table 1. The cellulolytic assay revealed that seven bacterial colonies of 16 colonies were showed positive results (TGBS01, TGBS05, TGBS07, TGBS09, TGBS10, TGBS13, and TGBS15). The highest zone of inhibition (20 mm) was observed in TGBS15 followed by TGBS09 (18 mm), TGBS01 (17 mm), and minimum (8 mm) in the strain TGBS13 in 24 h and 48 h zone of inhibition also observed and results showed that highest zone of inhibition (22 mm) was recorded in the strain TGBS15 and minimum (10 mm) in the strain TGBS13. There was no change in the zone of inhibition in the bacterial strain TGBS05 also noted. The efficiency of cellulolytic activity such as mean zone of diameter, mean colony diameter,

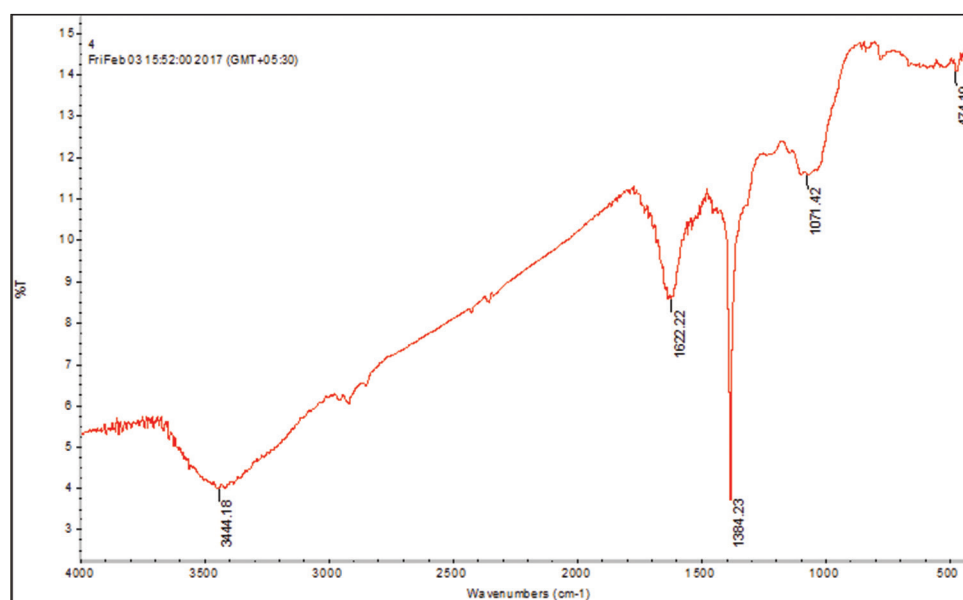


Figure 7: Fourier transform infrared image of silver nanoparticles synthesized by *Ceriops decandra*

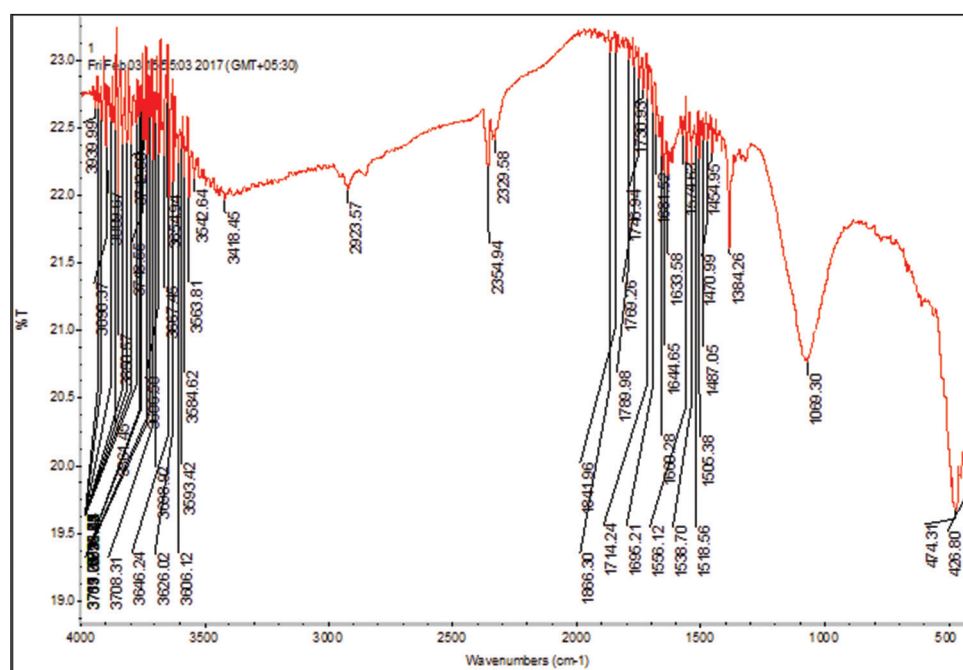


Figure 8: Fourier transform infrared image of silver nanoparticles synthesized by *Rhizophora mucronata*

Table 1: Isolated bacterial strains in three different dilutions from the gut of termite

Isolated bacterial colonies	Number of colonies (CFU/g)		
	10^{-3}	10^{-4}	10^{-5}
TGBS01	3	1	1
TGBS02	2	1	-
TGBS03	3	2	1
TGBS04	1	2	2
TGBS05	2	-	-
TGBS06	3	4	1
TGBS07	5	2	-
TGBS08	1	1	-
TGBS09	1	2	1
TGBS10	3	1	2
TGBS11	1	-	-
TGBS12	-	2	-
TGBS13	2	1	1
TGBS14	4	2	-
TGBS15	2	-	1
TGBS16	2	2	1

T: Termites, G: Gut, B: Bacteria, S: Serial number

clear zone, and ratio of the selected bacterial colonies was analyzed in 24 and 48 h and the results are depicted in Table 2. Mean zone of diameter is analyzed and separately noted in both 24 and 48 h. Maximum mean zone of diameter (20 and 22 mm) is recorded in strain TGBS15 and minimum (8 and 10 mm) in strain TGBS13 in both 24 and 48 h. The same patterns of results are also predicted in mean colony diameter (8 and 3 mm) in both 24 and 48 h. In 24 h, the highest clear zone (12 mm) is recorded in the strains TGBS09 and TGBS15 followed

Table 2: Antibacterial activity of biosynthesis silver nanoparticles of *Ceriops decandra* and *Rhizophora mucronata*

Bacterial isolates	Zone of inhibition (mm) in 24 h (μ g)					
	<i>Ceriops decandra</i>			<i>Rhizophora mucronata</i>		
	50	100	150	50	100	150
TGBS01	6	8	12	7	9	15
TGBS05	8	10	14	6	9	15
TGBS07	7	9	13	6	8	12
TGBS09	6	8	11	10	12	18
TGBS10	6	8	12	6	8	14
TGBS13	6	8	13	6	9	13
TGBS15	6	10	16	7	10	16

T: Termites, G: Gut, B: Bacteria, S: Serial number

by 11 mm in TGBS01, TGBS05, and lowest (5 mm) in TGBS13. Maximum clear zone (14 mm) is observed in the strain TGBS15 and minimum (7 mm) in TGBS13 of 48 h. No any changes are noted in the bacterial strain TGBS05 between 24 and 48 h. The deviation of clean zone results in all the strains for both 24 and 48 h is also represented in Table 3. Maximum zone of ratio is recorded in the strain TGBS05 (3.75 mm) followed by TGBS09 (3.00 mm) and minimum in TGBS07 (1.86 mm) for 24 h. In 48 h, the highest ratio of zone (3.75 mm) is noted in TGBS05 and low in TGBS07 (2.14 mm). The ratio zone variations of all the gut cellulolytic bacterial colonies for both 24 and 48 h are represented in Table 3. The isolated cellulolytic bacterial isolates were also examined to antibacterial assay with

Table 3: Efficiency of cellulolytic activity of isolated bacterial strains from the gut of termite

Isolated bacterial strains	Mean zone diameter (mm)		Mean colony diameter (mm)		Clear zone (mm)		Ratio	
	24 h	48 h	24 h	48 h	24 h	48 h	24 h	48 h
	TGBS01	17	19	6	6	11	13	2.83
TGBS05	15	15	4	4	11	11	3.75	3.75
TGBS07	13	15	7	7	6	8	1.86	2.14
TGBS09	18	20	6	6	12	14	3.00	3.33
TGBS10	14	15	5	5	9	10	2.80	3.00
TGBS13	08	10	3	3	05	07	2.66	3.33
TGBS15	20	22	8	8	12	14	2.50	2.75

T: Termites, G: Gut, B: Bacteria, S: Serial number

silver nanoparticles of the selected mangrove plants. The results indicated that *C. decandra* showed highest zone of inhibition with TGBS15 (6 mm⁻⁵⁰ µg, 10 mm⁻¹⁰⁰ µg, and 16 mm⁻¹⁵⁰ µg) and lowest zone of inhibition showed with TGBS09 (6 mm⁻⁵⁰ µg, 8 mm⁻¹⁰⁰ µg, and 11 mm⁻¹⁵⁰ µg) and *R. mucronata* showed highest zone of inhibition with TGBS09 (10 mm⁻⁵⁰ µg, 12 mm⁻¹⁰⁰ µg, and 18–150 µg) and lowest inhibition noted with TGBS07 (6 mm⁻⁵⁰ µg, 8 mm⁻¹⁰⁰ µg, and 12 mm⁻¹⁵⁰ µg). Comparatively, *R. mucronata* exhibited highest zone of inhibition of 18 mm at the concentration of 150 µg/disc and *C. decandra* showed highest zone of inhibition of 16 mm at the concentration of 150 µg/disc and results depicted in Table 2.

DISCUSSION

Termites are a major group of decomposers. They are playing a key role to decompose cellulose component present in wooden materials. They are lived rich in tropical and subtropical environments, where they involved beneficial help in breaking down and recycling one-third of the annual production of dead wood, on the other hand, also act as harmful pests which involved in destroying wood and wooden products of human homes, building materials, forests, and other commercial products, etc.^[19] In this study, 16 bacterial strains (TGBS01 to TGBS16) were isolated from the gut of the termite species *M. convolسیونarius*. Among these 16 bacterial strains, seven strains (TGBS01, TGBS05, TGBS07, TGBS09, TGBS10, TGBS13, and TGBS15) were screened as cellulolytic bacteria.^[26] Kakkar *et al.* (2015) have isolated 19 bacterial strains; of these, 15 strains exhibited

cellulolytic activity in the termite species *Odontotermes parvidens*. The similar results were also reported by Sharma *et al.*, 2015; Khiyami and Alyamani^[27,28] In general, UV-Vis spectroscopy can be used to observe size and shape of the controlled nanoparticles in aqueous suspense. The results of the UV-Vis absorption indicated increasing color intensity with increased time intervals and this might be due to the production of the silver nanoparticles^[29] and the formation of the brownish-yellow color might be due to the excitation of the surface plasmon vibration of the synthesized silver nanoparticles.^[30] The result of the XRD pattern indicates the presence of sharp bands of Bragg peaks and this might be due to the stabilization of the synthesized nanoparticles by the leaf extract of *R. mucronata* and *C. decandra* reducing agents and thus confirming the crystallization of the bioorganic phase occurs on the surface of the silver nanoparticles.^[31] The results of the FT-IR used to identify the possible biomolecules responsible for the stabilization of the synthesized silver nanoparticles. The result of this technique indicated the correspond values to the aliphatic group (cyclic CH₂-2 925.49), methyl group (CH₃-2 869.56), amide group (N-H stretching⁻³ 426.89), alkene (CC-1 631.49 and 669.178), alkane group (CH-2 346.95), and ether groups (COC-1 031.73). The formation of peaks may be considered as major functional groups in various chemical classes such as flavonoids, triterpenoids, and polyphenols.^[2] Hence, the terpenoids are confirmed to have better potential activity in the metal ions to convert the aldehyde groups to carboxylic acids. In addition, amide groups are also inducing for the available of the enzymes and these enzymes are helping for the reduction synthesis and stabilization of the metal ions. Besides, polyphenols are also proved to have potential reducing agent in the biosynthesis of the silver nanoparticles.^[20]

In this study, the isolated cellulolytic gut bacterial strains are subjected to antibacterial assay with synthesized nanoparticles of two mangrove plants *C. decandra* and *R. mucronata*. The biosynthesized nanoparticles were prepared at three different concentrations of 50, 100, and 150 µg/disc, respectively. The disc diffusion method was carried out on antibacterial assay with all the seven cellulolytic gut bacterial strains. Among these two plants synthesized nanoparticles, the better and

prominent results are predicted in *R. mucronata* when compared to *C. decandra*. Our results also confirmed by Upadhyaya *et al.*^[32] have stated that *R. mucronata* AgNPs indicated that maximum zone was shown as 16 mm, 14 mm, and 14 mm for *Pseudomonas floescence*, *Proteus* spp., and *Flavobacterium* spp., respectively, at 75 µg/µL concentrations. In addition,^[21] Gnanadesigan *et al.*(2011) have also recorded that the biosynthesized silver nanoparticles of the leaf extract of *R. mucronata* provided potential killing effect of mosquito larvae. The present findings are finally concluded that the biosynthesized silver nanoparticles of the leaf extract of *R. mucronata* revealed possible potential effect against gut cellulolytic bacteria and it could be also used as potential drug to anti-termite activity.

REFERENCES

- Ankamwar B, Damle C, Ahmad A, Sastry M. Biosynthesis of gold and silver nanoparticles using *Emblica officinalis* fruit extract, their phase transfer and transmetallation in an organic solution. *J Nanosci Nanotechnol* 2005;5:1665-71.
- Nabikhan A, Kandasamy K, Raj A, Alikunhi NM. Synthesis of antimicrobial silver nanoparticles by callus and leaf extracts from saltmarsh plant, *Sesuvium portulacastrum* L. *Colloids Surf B Biointerfaces* 2010; 79:488-93.
- Bultman JD, Beal RH, Ampong FF. Natural resistance of some tropical African woods to *Coptotermes formosanus* Shiraki. *For Prod J* 1979;29:46-51.
- Carter FL, Garlo AM, Stanely JB. Termiticidal components of wood extracts: 7 methyljuglone from *Diospyros virginiana*. *J Agri Food Chem* 1978; 26:869-73.
- FAO and UNEP. Termite Biology and Management Workshop. Vol. 46. Geneva: UNEP, Vetenskapsakademiens Handlingar; 2000. p. 1-88.
- Bose G. Termite fauna of southern India. *Rec Zool Sur Ind* 1984;49:1-270.
- Gnanadesigan M, Anand M, Ravikumar S, Maruthupandy M, Vijayakumar V, Selvam S, *et al.* Biosynthesis of silver nanoparticles by using mangrove plant extract and their potential mosquito larvicidal property. *Asian Pac J Trop Med* 2011;4:799-803.
- Govindappa M, Farheen H, Chandrappa CP, Channabasava, Ravishankar VR, Vinay BR. Mycosynthesis of silver nanoparticles using extract of endophytic fungi *Penicillium* species of *Glycosmis mauritiana* and its antioxidant, antimicrobial, anti-inflammatory and tyrokinase inhibitory activity. *Adv Nat Sci Nanosci Nanotechnol* 2016;7:1-9.
- Holt JA, Lepage M. Termites and soil properties. In: *Termites: Evolution, Sociality, Symbiosis, Ecology*. Netherlands: Springer, Dordrecht; 2017. p. 389-407.
- Jayaseelan C, Rahuman AA, Rajakumar G, Vishnu Kirthi A, Santhoshkumar T, Marimuthu S, *et al.* Synthesis of pedicelocidal and larvicidal silver nanoparticles by leaf extract from heartleaf moonseed plant, *Tinospora cordifolia* Miers. *Parasitol Res* 2011; 109:185-94.
- Joshi PK, Singh NP, Singh NN, Roberta VG, Prabhu PL. Maize in India: Production Systems. Mexico: Constraints and Research Priorities, D.F. CIMMYT; 2005. p. 22.
- Kakkar N, Sanjeev KG, Baljeet SS. Studies on cellulolytic activity and structure of symbiotic bacterial community in *Odontotermes parvidens* Guts. *Int J Curr Microbiol Appl Sci* 2015;4:310-5.
- Kasthuri J, Kathiravan K, Rajendran N. Phyllanthin assisted biosynthesis of silver and gold nanoparticles a novel biological approach. *J Nanopart Res* 2009; 11:1075-85.
- Khiyami M, Alyamani E. Aerobic and facultative anaerobic bacteria from gut of red palm weevil (*Rhynchophorus ferrugineus*). *Afri J Biotechnol* 2008; 7:1432-7.
- Krishnaraj C, Jagan EG, Rajasekar S, Selvakumar P, Kalaichelvan PT, Mohan N, *et al.* Synthesis of silver nanoparticles using *Acalypha indica* leaf extracts and its antibacterial activity against water borne pathogens. *Colloids Surf B Biointerfaces* 2010;76:50-6.
- Kumar VA, Uchida T, Mizuki T, Nakajima Y, Katsube Y, Hanajiri T, *et al.* Synthesis of nanoparticles composed of silver and silver chloride for a plasmonic photocatalyst using an extract from a weed *Solidago altissima* (goldenrod). *Adv Nat Sci Nanosci Nanotechnol* 2016; 7:1-12.
- Gavade SJ, Nikam GH, Dhabbe RS, Sabale SR, Tamhankar BV, Mulik GN. Green synthesis of silver nanoparticles by using carambola fruit extract and their antibacterial activity. *Adv Nat Sci Nanosci Nanotechnol* 2015;6:45015.
- Masurkar SA, Chaudhari PR, Shidore VB, Kamble SP. Effect of biosynthesized silver nanoparticles on *Staphylococcus aureus* biofilm quenching and prevention of biofilm formation. *Nano Micro Lett* 2012;4:34-9.
- Meyer JR. Isoptera. Department of Entomology. NC State University; 2005. Available from: <https://www.cals.ncsu.edu/entomology-and-plant-pathology>.
- Mukunthan KS, Elumalai EK, Patel TN, Murty VR. *Catharanthus roseus*: A natural source for the synthesis of silver nanoparticles. *Asian Pac J Trop Biomed* 2011; 1:270-4.
- Parashar UK, Saxena PS, Srivastava A. Bioinspired synthesis of silver nanoparticles. *Dig J Nanomater Biostruct* 2009;4:159-66.
- Premalatha K, Rajavel DS. Termite fauna of Southern Tamil Nadu. In: *Abstracts of 98th Indian Science Congress*. Chennai: SRM University; 2011. p. 1-80.
- Rajagopal D. Economically important termite species in India. *Sociobiology* 2002;41:33-46.
- Rasplus JY, Roques A. *Dictyoptera (Blattodea, Isoptera), Orthoptera, Phasmatodea and Dermaptera* chapter 13.3. *Bio Risk Biodivers Ecosyst Risk Assess* 2010;4:807-31.

25. Ravikumar S, Vinoth R, Selvan GP. Bioactive potential of Seagrass *Syringodium isoetifolium* against fish pathogens. J Pharm Res 2011;4:1854-6.
26. Saeki I, Sumimoto M, Kondo T. The termiticidal substances from the wood *Chamaecyparis pisifera* D. Don. Holzforschung 1973;27:93-6.
27. Scheffrahn RH, Hsu RC, Su NY, Huffman JB, Midland SL, Sims JJ, *et al.* Allelochemical resistance of bald cypress, *Taxodium distichum*, heartwood to the subterranean termite, *Coptotermes formosanus*. J Chem Ecol 1988;14:765-76.
28. Sharma D, Joshi B, Bhatt MR, Joshi J, Malla R, Bhattarai T, *et al.* Isolation of cellulolytic organisms from the gut contents of termites native to nepal and their utility in saccharification and fermentation of lignocellulosic biomass. J Bio Biofuel 2015;2: 11-20.
29. Shrivastava S, Dash D. Label-free colorimetric estimation of proteins using nanoparticles of silver. Nano-Micro Lett 2010;2:164-8.
30. Su NY. Novel technologies for subterranean termite control. Sociobiology 2002;40:95-101.
31. Sugimoto A, Bignell DE, Macdonald JA. Global impact of termites on the carbon cycle and atmospheric trace gases. In: Termites: Evolution, Sociality, Symbioses, Ecology. Berlin: Springer; 2000. p. 409-35.
32. Umashankari J, Inbakandan D, Ajithkumar TT, Balasubramanian T. Mangrove plant, *Rhizophora mucronata* (Lamk, 1804) mediated one pot green synthesis of silver nanoparticles and its antibacterial activity against aquatic pathogens. Aquat Biosyst 2012;8:1-11.
33. Upadhyaya R, Jaiswal G, Ahmad S, Khanna L, Jain SC. Antitermite activities of *C. decidua* extracts and pure compounds against Indian white termite *Odontotermes obesus* (Isoptera: Odontotermitidae). A J Entomol 2012;1:1-9.